

Expression of the zinc finger transcription factor zDC (Zbtb46, Btbd4) defines the classical dendritic cell lineage

Matthew M. Meredith,¹ Kang Liu,⁴ Guillaume Darrasse-Jeze,⁵ Alice O. Kamphorst,^{1,6} Heidi A. Schreiber,¹ Pierre Guermonprez,¹ Juliana Idoyaga,² Cheolho Cheong,² Kai-Hui Yao,¹ Rachel E. Niec,⁷ and Michel C. Nussenzweig^{1,3}

¹Laboratory of Molecular Immunology, ²Laboratory of Cellular Physiology and Immunology, and ³Howard Hughes Medical Institute, The Rockefeller University, New York, NY 10065

⁴Department of Microbiology and Immunology, Columbia University, New York, NY 10027

⁵Department of Biotherapy, Institut National de la Santé et de la Recherche Médicale, Faculte de meidecine, Universite Paris Descartes, Sorbonne Paris Citei, Paris F-75015, France

⁶Emory Vaccine Center, Emory University School of Medicine, Atlanta, GA 30329

⁷Immunology Program, Memorial Sloan-Kettering Cancer Center, New York, NY 10065

Classical dendritic cells (cDCs), monocytes, and plasmacytoid DCs (pDCs) arise from a common bone marrow precursor (macrophage and DC progenitors [MDPs]) and express many of the same surface markers, including CD11c. We describe a previously uncharacterized zinc finger transcription factor, zDC (Zbtb46, Btbd4), which is specifically expressed by cDCs and committed cDC precursors but not by monocytes, pDCs, or other immune cell populations. We inserted diphtheria toxin (DT) receptor (DTR) cDNA into the 3' UTR of the zDC locus to serve as an indicator of zDC expression and as a means to specifically deplete cDCs. Mice bearing this knockin express DTR in cDCs but not other immune cell populations, and DT injection into zDC-DTR bone marrow chimeras results in cDC depletion. In contrast to previously characterized CD11c-DTR mice, non-cDCs, including pDCs, monocytes, macrophages, and NK cells, were spared after DT injection in zDC-DTR mice. We compared immune responses to *Toxoplasma gondii* and MO4 melanoma in DT-treated zDC- and CD11c-DTR mice and found that immunity was only partially impaired in zDC-DTR mice. Our results indicate that CD11c-expressing non-cDCs make significant contributions to initiating immunity to parasites and tumors.

CORRESPONDENCE

Michel C. Nussenzweig:
nussen@rockefeller.edu

Abbreviations used: Ad-OVA, OVA-expressing adenovirus; cDC, classical DC; CDP, common DC progenitor; DT, diphtheria toxin; DTR, DT receptor; mDC, migratory DC; MDP, macrophage and DC progenitor; mLN, mesenteric LN; MLR, mixed leukocyte reaction; MP, myeloid progenitor; pDC, plasmacytoid DC; skLN, skin-draining LN; UTR, untranslated region.

DCs were discovered because of their distinct morphology (Steinman and Cohn, 1973) and were further distinguished from macrophages based on cell surface features (Nussenzweig et al., 1981, 1982) and their superior ability to present antigen (Nussenzweig et al., 1980; Banchereau and Steinman, 1998). Like other myeloid cells, classical DCs (cDCs) develop in the bone marrow from myeloid progenitors (MPs) that give rise to specialized precursors, macrophage and DC progenitors (MDPs), that are restricted to produce monocytes, plasmacytoid DCs (pDCs), and cDCs (Fogg et al., 2006; Varol et al., 2007). The monocyte and cDC development pathways separate when MDPs give rise to common DC progenitors (CDPs), which produce pDCs and cDCs but not monocytes (Naik et al., 2007; Onai et al., 2007; Liu

et al., 2009). Finally, CDPs differentiate into pre-DCs, fully committed cDC precursors which produce cDCs but do not demonstrate monocyte or pDC potential (Naik et al., 2006; Liu et al., 2009).

After development in the bone marrow, pre-DCs travel via the blood to lymphoid and nonlymphoid tissues where they undergo Flt3L-dependent expansion and differentiate into cDCs (Liu et al., 2007; Waskow et al., 2008; Bogunovic et al., 2009; Ginhoux et al., 2009; Liu et al., 2009). The Flt3L-dependent pre-DC pathway is the predominant means for cDC

© 2012 Meredith et al. This article is distributed under the terms of an Attribution-Noncommercial-Share Alike-No Mirror Sites license for the first six months after the publication date (see <http://www.rupress.org/terms>). After six months it is available under a Creative Commons License (Attribution-Noncommercial-Share Alike 3.0 Unported license, as described at <http://creativecommons.org/licenses/by-nc-sa/3.0/>).

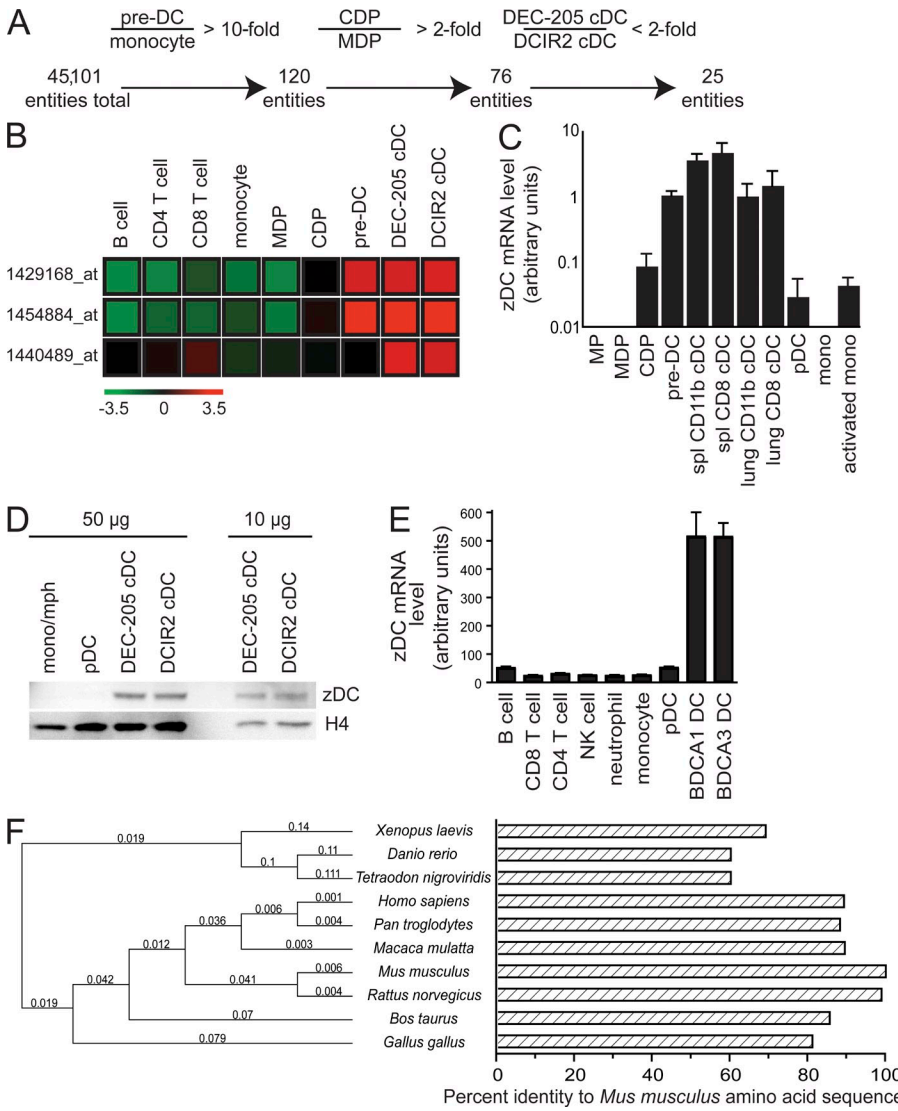


Figure 1. zDC expression is specific to cDCs. (A) Analysis of gene array data of mouse DEC-205⁺ (CD8⁺) cDCs, DCIR2⁺ (CD4⁺) cDCs, pre-DCs, CDPs, MDPs, and monocytes. (B) Heat maps showing normalized zDC expression depicted on \log_2 scale from three zDC probes on Affymetrix 430 2.0 chips. All populations were prepared in triplicate. (C) zDC transcript levels in mouse MPs, MDPs, CDPs, pre-DCs, splenic and lung cDC subsets, pDCs, and steady-state and activated monocytes determined by Q-PCR and normalized to GAPDH. All populations were prepared in triplicate and error bars indicate SEM. (D) zDC Western blot of mouse CD11b-enriched monocytes/macrophages, PDCA-1-enriched pDCs, and sorted DEC-205⁺ and DCIR2⁺ cDCs. Histone H4 blot is shown as a loading control. The blot represents one experiment of three with equivalent results. Diluted cDC lysates (10 µg) are included to show that zDC protein is still detectable even with limited cell lysate input. (E) Gene array expression of human ZDC (probe 227329_at on Affymetrix U133 Plus 2.0) by sorted human blood populations. Error bars indicate SEM. This panel was adapted with permission from Robbins et al. (2008). (F) Dendrogram of vertebrate zDC amino acid sequences (left) and percent identity to mouse (right).

development in the steady state *in vivo* (Karsunky et al., 2003; Naik et al., 2005; Waskow et al., 2008). Pre-DC differentiation produces both major cDC subsets in lymphoid tissues (CD8⁺DEC205⁺ and CD4⁺DCIR2⁺ cDCs), as well as CD103⁺ cDC and some CD11b⁺CD103[−] cDC in nonlymphoid tissues (Naik et al., 2006; Ginhoux et al., 2009; Helft et al., 2010).

Cells with many of the phenotypic characteristics of cDCs, i.e., high levels of CD11c and MHCII expression, can also develop from monocytes cultured with GM-CSF and IL-4 *in vitro* (Romani et al., 1994; Sallusto and Lanzavecchia, 1994; Sallusto et al., 1995). Furthermore, monocytes can express high levels of CD11c and MHCII when they are activated in the context of several inflammatory conditions *in vivo* (Serbina et al., 2003; León et al., 2007; Hohl et al., 2009). Like cDCs, activated monocytes can present antigen *in vitro* and *in vivo*, especially after stimulation by TLR ligands (Randolph et al., 2008; Kamphorst et al., 2010). This convergence in phenotype between cDCs and monocytes/

macrophages has made it difficult to distinguish these cell types and to determine their individual contributions to immune responses *in vivo* (Hashimoto et al., 2011). For example, the CD11c-diphtheria toxin (DT) receptor (DTR) mouse model, which has been used extensively to study the function of cDCs *in vivo*, cannot definitively distinguish cDCs from other CD11c-expressing cells including macrophages, activated monocytes, and pDCs (Probst et al., 2005; Zammit et al., 2005; Bennett and Clausen, 2007; Murphy, 2011).

Here, we identify a zinc finger transcription factor, zDC, which is evolutionarily conserved and specifically expressed by cDC but not monocytes or other immune populations. We describe the production of a knockin mouse wherein DTR expression is placed under the control of the zDC locus (zDC-DTR), and we compare the effects of DT treatment in zDC- and CD11c-DTR mice on immune cells and immunization *in vivo*.

RESULTS

zDC expression is restricted to cDCs

To identify gene loci specifically expressed by cDCs, we performed gene array analysis comparing developing and fully differentiated cDCs with monocytes and myeloid cell progenitors (Fogg et al., 2006; Onai et al., 2007; Liu et al.,

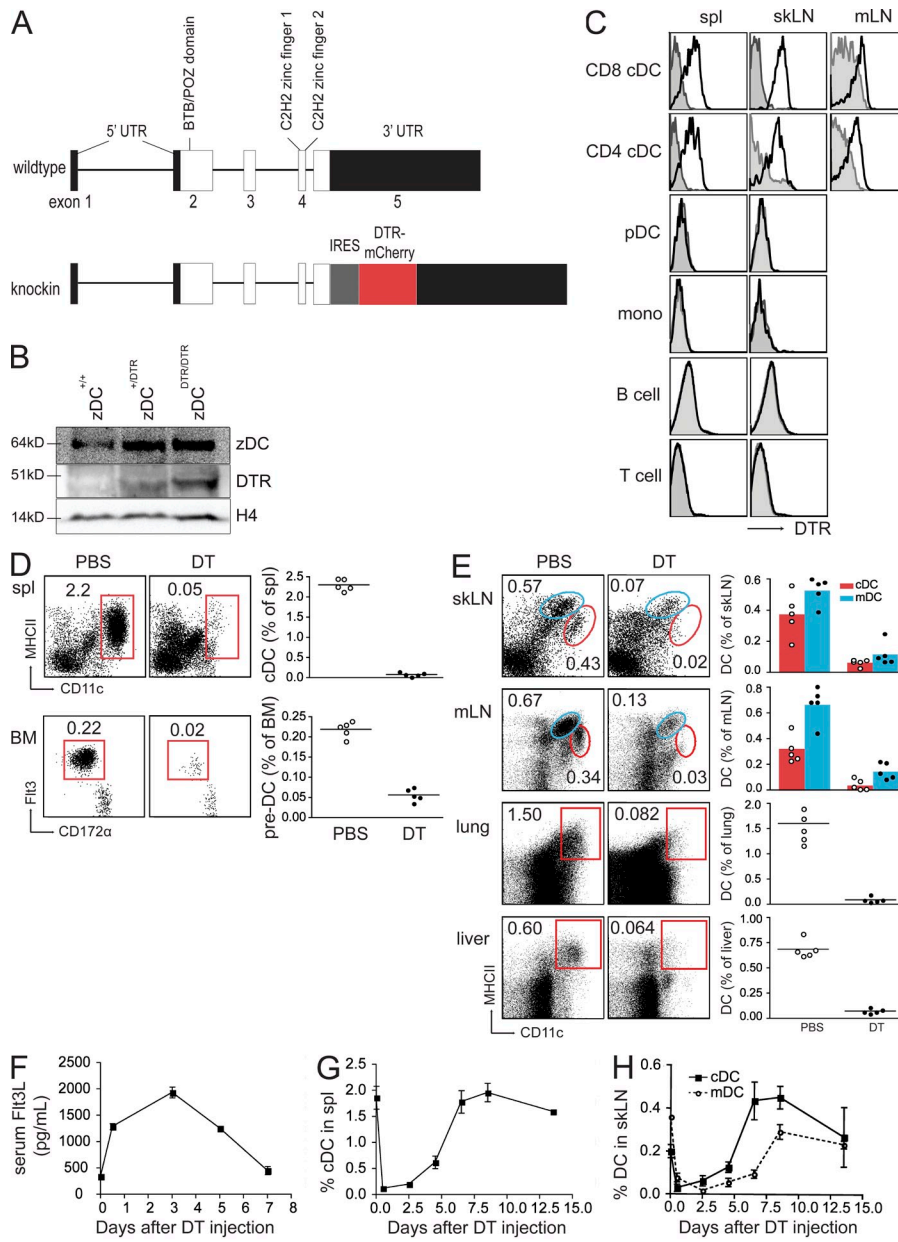


Figure 2. DTR expression regulated by the zDC locus permits DT ablation of cDCs. (A) Schematic diagram of wild-type and DTR knockin zDC loci. 5' and 3' UTR are shown in black, coding sequences in white, and the locations of BTB/POZ and zinc finger domains are indicated. IRES (gray) and DTR-mCherry (red) are inserted immediately after the endogenous zDC stop codon in exon 5. (B) Western blots for zDC, hDTR, and Histone H4 (loading control) on CD11c-enriched splenocytes from zDC^{+/+}, zDC^{+/DTR}, and zDC^{DTR/DTR} mice. (C) Flow cytometry histograms of DTR staining by CD8⁺ and CD4⁺ cDCs (Lin⁻Ly6C⁻CD11c⁺ MHCII⁺), pDCs (Lin⁻CD11c^{int}PDCA-1⁺), monocytes (Lin⁻CD11b⁺CD115⁺), B cells (CD3⁻NK1.1⁻CD19⁺), and T cells (CD3⁺CD19⁻NK1.1⁻) from the spleens (spl), skLN, and mLN of zDC-DTR mice (black line) and wild-type littermates (gray shaded). (D) Flow cytometry plots of splenocytes (gated on Lin⁻) and bone marrow pre-DCs (gated on Lin⁻CD45R⁻CD11c⁺MHCII⁻) in zDC-DTR bone marrow chimeras injected with PBS or DT. Numbers indicate percentage of organ. Graphs on right represent three to four experiments with each point representing one mouse and horizontal lines representing the means. (E) CD11c^{hi}MHCII⁺ cDC and CD11c⁺MHCII^{hi} mDC abundance in skLN, mLN, lung, and liver in PBS- and DT-treated zDC-DTR bone marrow chimeras, gated on Lin⁻ in skLN and mLN, and Lin⁻CD45⁺ in liver and lung. (F) Fit3L concentrations in sera of DT-treated zDC-DTR bone marrow chimeras determined by ELISA at multiple time points after DT injection. (G and H) cDC abundance in spleen (G) and skLN (H) at multiple time points after DT injection. Results represent two to three experiments with two to three mice per group per experiment. Error bars indicate SEM. Lin⁻; CD3⁻CD19⁻NK1.1⁻.

2009; Fig. 1 A). We found a previously uncharacterized zinc finger transcription factor we call zDC (Zbtb46, Btbd4), which was specifically expressed by pre-DCs and cDCs. Gene array analysis and quantitative PCR (Q-PCR) validation demonstrated that bone marrow pre-DCs and cDCs from both spleen and lung expressed 10-fold greater levels of zDC transcript compared with bone marrow MPs, MDPs, CDPs, pDCs, steady-state and activated monocytes, and lymphocytes (Fig. 1, B and C). We further confirmed this pattern of cDC-specific expression using public online gene array databases (immgene.org and biogps.org).

To determine whether cDCs express zDC protein, we produced a hamster monoclonal antibody against zDC and performed Western blotting on monocyte/macrophage, pDC, and cDC cell lysates. Consistent with our mRNA expression

data, zDC protein was detected in cDCs but not pDCs or monocytes (Fig. 1 D). Furthermore, the expression of human ZDC is also limited to human cDCs (Robbins et al., 2008; Fig. 1 E). Finally, zDC is highly conserved throughout vertebrate evolution but not found in cartilaginous fish (Fig. 1 F). We conclude that zDC expression is up-regulated and maintained after the CDP stage in development when the cDC lineage splits from monocytes and pDCs (Liu et al., 2009), and that among bone marrow-derived cells its steady-state expression is restricted to cDCs.

zDC-DTR mice

To further explore zDC regulation and exploit its cDC-specific expression pattern, we introduced a cDNA encoding human DTR into the 3' untranslated region (UTR) of the zDC

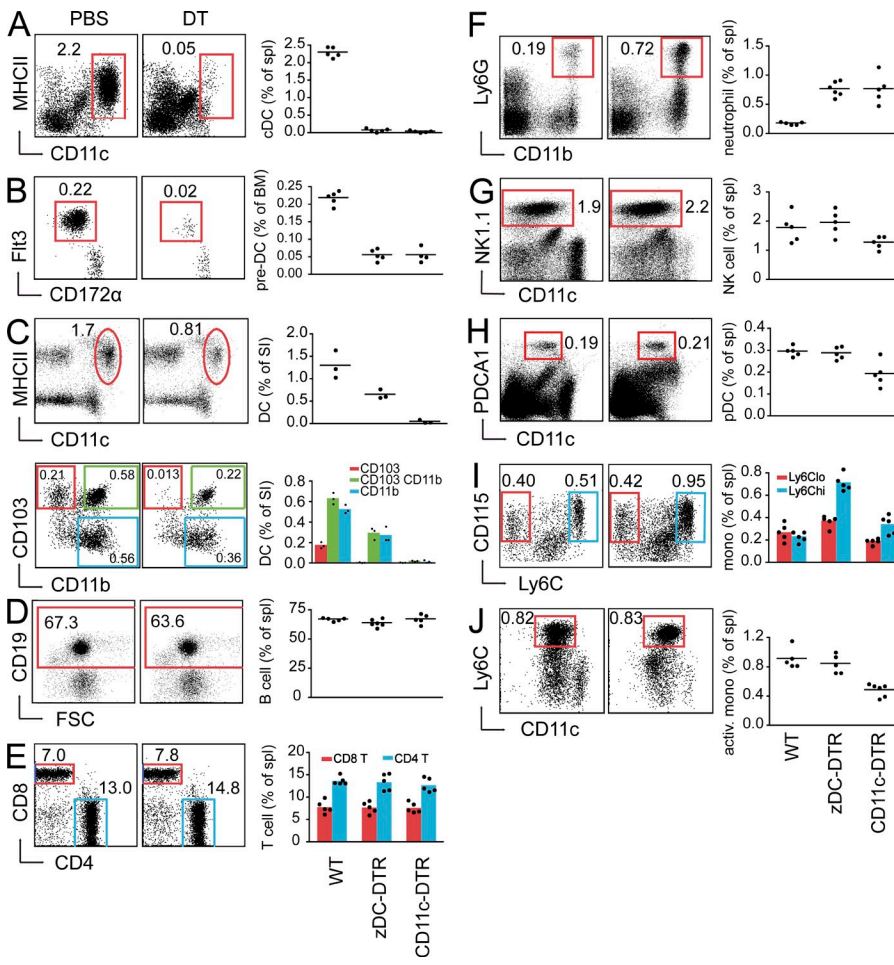


Figure 3. DT ablation in zDC-DTR bone marrow chimeras is specific to cDCs and spares other CD11c-expressing cells.

(A–I) Steady-state splenic cDCs (A) and bone marrow pre-DCs (B; as defined in Fig. 2 D), CD45⁺CD3[−]B220[−]CD11c^{hi}MHCII⁺ small intestine (SI) lamina propria DCs (C, top) and DC subsets (C, bottom), CD19⁺ splenic B cells (D), CD19[−]NK1.1[−]CD3⁺ T cells (E), Lin[−]CD11b⁺Ly6G⁺ neutrophils (F), CD3[−]CD19[−]NK1.1⁺ NK cells (G), Lin[−]CD11c^{int}PDCA-1⁺ pDCs (H), and Lin[−]Flt3[−]CD11b⁺Ly6G[−]CD115⁺ monocytes (I) in PBS- or DT-treated steady-state zDC-DTR bone marrow chimeras. Results represent three to four experiments. (J) Lin[−]CD11b⁺Ly6G[−]CD11c⁺Ly6C⁺ activated monocytes in PBS- or DT-treated *L. monocytogenes*-infected zDC-DTR bone marrow chimeras. Graphs on the right show percentage of indicated population in DT-treated WT, zDC-DTR, and CD11c-DTR bone marrow chimeras with each point representing one mouse and horizontal lines showing the mean per group.

restricted to cDC; however, it is also expressed by a yet unknown group of essential radioresistant cells.

To determine which bone marrow-derived cells are sensitive to DT, we injected zDC-DTR \rightarrow C57BL/6 bone marrow chimeras with DT and measured the effects by flow cytometry. Splenic cDCs and bone mar-

row pre-DCs were ablated as early as 12 h after DT injection (Fig. 2 D). In addition to the spleen, cDCs in the skLN, mLN, lung, and liver were equally sensitive to DT ablation (Fig. 2 E). Furthermore, CD11c⁺MHCII^{hi} migratory DC (mDC) found in skLNs and mLNs were similarly decreased after DT treatment. Like CD11c-DTR (Schmid et al., 2011), DT injection into zDC-DTR \rightarrow C57BL/6 bone marrow chimeras resulted in a rapid fourfold increase in serum Flt3L concentration which returned to steady-state levels after 7 d (Fig. 2 F). Consistent with the increased serum Flt3L and the kinetics of cDC development (Liu et al., 2007, 2009; Waskow et al., 2008), cDC reconstitution in the spleen was apparent as early as 5 d after DT injection and was complete after 7 d (Fig. 2 G), which is similar to the kinetics observed after ablation in CD11c-DTR mice (Jung et al., 2002). cDC reconstitution in the skLNs was similar to splenic cDC reconstitution, whereas mDC kinetics were delayed by about 2 d (Fig. 2 H). We conclude that DT injection into zDC-DTR bone marrow chimeras results in efficient ablation of pre-DCs and their progeny in lymphoid and nonlymphoid tissue throughout the organism.

Similar to CD11c-DTR (Zaft et al., 2005), an essential radioresistant population must also express zDC because injection of a single dose of 20 ng DT per gram of body weight into zDC-DTR knockin mice and C57BL/6 \rightarrow zDC-DTR bone marrow chimeras is fatal within 24–48 h. Conversely, zDC-DTR \rightarrow C57BL/6 bone marrow chimeras survive DT injections every other day for >2 wk. Thus, among bone marrow-derived cells, zDC-DTR expression appears to be

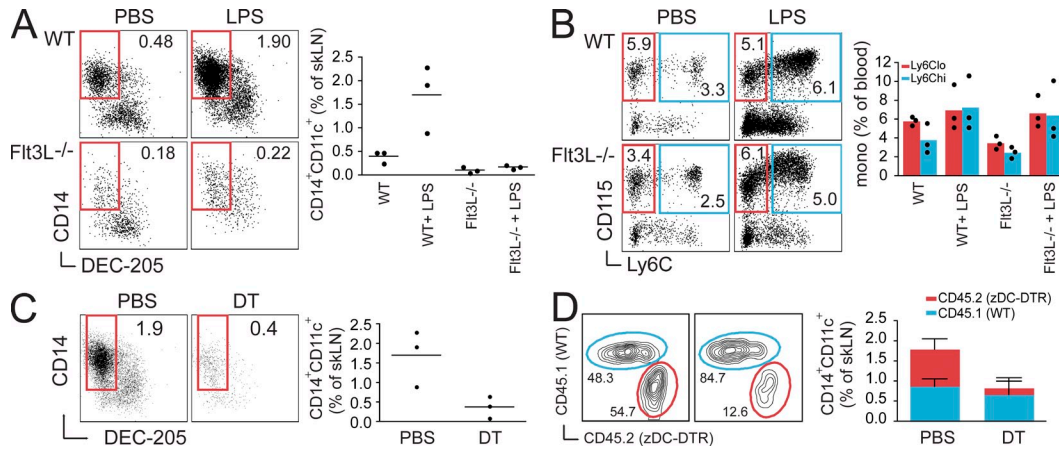


Figure 4. CD11c⁺CD14⁺ cells in skLNs derive from cDCs. (A and B) CD11c⁺MHCII⁺CD14⁺ cells in skLN (A) and Lin⁻Flt3⁻CD11b⁺Ly6G⁻CD115⁺ monocytes (B) in blood 24 h after PBS or LPS injection in WT and Flt3L^{-/-} mice. Graphs on the right summarize three experiments, with each point representing one mouse and the horizontal bars showing the mean. (C) CD11c⁺MHCII⁺CD14⁺ cells in skLN 24 h after LPS injection in PBS- or DT-treated zDC-DTR bone marrow chimeras. (D) CD45.1⁺ WT versus CD45.2⁺ zDC-DTR contribution to CD11c⁺MHCII⁺CD14⁺ cells in skLN 24 h after LPS treatment in PBS- or DT-treated WT:zDC-DTR mixed bone marrow chimeras. Error bars indicate SEM.

DT ablation in zDC- and CD11c-DTR bone marrow chimeras resulted in equivalent loss of splenic cDCs and bone marrow pre-DCs within 12 h of injection (Fig. 3, A and B). Although splenic cDCs originate from pre-DC precursors, DCs in some nonlymphoid tissues can arise from pre-DCs or monocytes (Helft et al., 2010; Liu and Nussenzweig, 2010). For example, in the small intestine, CD103⁺ cDCs are derived exclusively from pre-DCs, whereas CD11b⁺ DCs can arise from either pre-DCs or monocytes (Bogunovic et al., 2009; Varol et al., 2009). As a result of this monocyte contribution, DT treatment in zDC-DTR bone marrow chimeras resulted in only a partial reduction of CD11c^{hi}MHCII⁺ DCs in the small intestine lamina propria (Fig. 3 C). Specifically, pre-DC-derived CD103⁺CD11b⁻ cDCs were completely depleted in the lamina propria, whereas only a portion of CD103⁺CD11b⁺ and CD103⁻CD11b⁺ DCs were affected by DT treatment (Fig. 3 C). DT treatment in CD11c-DTR bone marrow chimeras, however, resulted in a complete ablation of all CD11c^{hi}MHCII⁺ DCs regardless of pre-DC or monocyte origin (Fig. 3 C). Therefore, DT treatment in zDC-DTR bone marrow chimeras ablates pre-DC-derived cDCs, while leaving monocyte-derived populations intact.

To understand what effect DT treatment has on non-cDC populations in DT-treated zDC- and CD11c-DTR bone marrow chimeras, we looked for changes in other lymphoid and myeloid populations. As a result of the absence of zDC and CD11c expression, steady-state B and T lymphocytes were unaffected by DT injection in both zDC- and CD11c-DTR chimeras (Fig. 3, D and E). Although activated T cells can up-regulate CD11c, which renders them sensitive to DT treatment in CD11c-DTR mice (Jung et al., 2002; Bennett and Clausen, 2007), zDC expression remains low in activated T cells (immgen.org). Additionally, both zDC- and CD11c-DTR chimeras showed increased numbers of splenic Ly6G⁺ neutrophils after DT injection (Tittel et al., 2012; Fig. 3 F).

Moreover, whereas NK cells and pDCs were unaffected by DT injection in zDC-DTR bone marrow chimeras, both of these populations were reduced in DT-treated CD11c-DTR chimeras (Fig. 3, G and H). pDCs activated with the TLR9 ligand CpG, which up-regulates MHCII and co-stimulatory receptor expression (Iparraguirre et al., 2008), were likewise unaffected by DT treatment in zDC-DTR mice (unpublished data). Thus, the intermediate levels of CD11c expressed by NK cells and pDCs must be sufficient to induce depletion of these populations after DT treatment in CD11c-DTR mice.

In addition to NK cells and pDCs, Ly6C^{lo} monocytes also express low levels of CD11c. Consequently, whereas DT treatment in zDC-DTR resulted in a small increase in Ly6C^{lo} monocyte numbers, this monocyte subset is reduced by DT treatment in CD11c-DTR chimeras (Fig. 3 I). As might be expected, the number of Ly6C^{hi} monocytes, which do not express CD11c in the steady state, increased after DT treatment in both zDC- and CD11c-DTR chimeras (Fig. 3 I). We conclude that cDC depletion by DT treatment in the steady state is far more specific in zDC- than in CD11c-DTR mice.

Activation of Ly6C^{hi} monocytes during infection or by stimulation in vitro with cytokines and TLR ligands induces CD11c and MHCII expression (Randolph et al., 1999; Geissmann et al., 2003; Gordon and Taylor, 2005). For example, during infection with *Listeria monocytogenes*, Ly6C^{hi} monocytes accumulate in the spleen and up-regulate CD11c, MHCII, and co-stimulatory markers (Serbina et al., 2003). Because this population also produces TNF and iNOS, they are also referred to as tipDCs. Consistent with the increase in CD11c expression by these activated monocytes, DT treatment in CD11c-DTR chimeras during *L. monocytogenes* infection reduces the proportion of this population in the spleens of infected mice by ~50% (Fig. 3 J). In contrast, the

number of activated CD11c⁺Ly6C^{hi} monocytes is not altered by DT treatment in zDC-DTR chimeras.

Additional populations of CD11c⁺MHCII⁺ cells appear in lymphoid organs during inflammation, and it has been difficult to ascertain their origin from pre-DCs or monocytes. For example, LPS injection results in the appearance of CD11c⁺MHCII⁺DC-SIGN/CD209⁺CD14⁺ cells in skLNs. Although initially attributed to monocyte origin (Cheong et al., 2010), these cells fail to accumulate after LPS injection in Flt3L^{-/-} mice (Fig. 4 A) despite the presence of normal blood monocyte numbers (Fig. 4 B), suggesting they arise from cDCs and not from monocytes. Consistent with this hypothesis, zDC-DTR mice treated with DT 24 h before LPS injection lacked CD11c⁺MHCII⁺CD14⁺DEC-205⁻ cells in skLNs (Fig. 4 C). However, the lack of CD11c⁺MHCII⁺DC-SIGN/CD209⁺CD14⁺ cell accumulation in Flt3L^{-/-} and DT-treated zDC-DTR mice could also occur as a result of the absence of cDC-derived help. To address this possibility, we looked at CD11c⁺MHCII⁺DC-SIGN/CD209⁺CD14⁺ cell accumulation after LPS injection in PBS- and DT-treated CD45.1⁺WT:CD45.2⁺zDC-DTR mixed bone marrow chimeras which maintain DT-insensitive CD45.1⁺WT cDCs after DT injection. Although DT-treated mixed bone marrow chimeras were able to generate CD45.1⁺WT CD11c⁺MHCII⁺DC-SIGN/CD209⁺CD14⁺ cells, few were derived from CD45.2⁺zDC-DTR cells (Fig. 4 D). We conclude that CD11c⁺MHCII⁺DC-SIGN/CD209⁺CD14⁺ should be categorized as activated cDCs and that they are not of monocyte origin. Thus, during inflammation, DT treatment in zDC-DTR bone marrow chimeras depletes cDCs but spares activated monocytes that express CD11c and MHCII, whereas DT treatment in CD11c-DTR mice depletes both cell types.

Like their monocyte precursors, many macrophage subsets express low levels of CD11c and have been shown to be sensitive to DT ablation in CD11c-DTR mice (Bennett and Clausen, 2007). For example, splenic red pulp macrophages are depleted in DT-treated CD11c-DTR bone marrow chimeras (Fig. 5 A). In contrast, this population is maintained in zDC-DTR bone marrow chimeras. Although a previous study had concluded that F4/80⁺ red pulp macrophages are maintained as a result of the presence of CD11b⁺ cells in the spleen, these cells more likely represent CD11b⁺ neutrophil infiltration (Tittel et al., 2012) and not red pulp macrophages which are CD11b^{lo/-} (Kohyama et al., 2009).

To better characterize macrophage populations, we performed immunohistochemistry experiments on DT-treated zDC-DTR knockin and CD11c-DTR hemizygous mice because reconstitution of macrophage populations is incomplete in bone marrow chimeras (Schulz et al., 2012). In agreement with our analysis by flow cytometry, splenic F4/80⁺ red pulp macrophages were unaffected by DT treatment in zDC-DTR mice and absent in CD11c-DTR mice (Fig. 5 B). Similarly, CD169⁺ marginal zone macrophages in the spleen were present after DT treatment in zDC-DTR mice, whereas this population was almost absent in DT-treated CD11c-DTR

mice (Fig. 5 C). In the skLN, F4/80⁺ medullar macrophages appeared unaffected by DT treatment in both zDC- and CD11c-DTR mice (Fig. 5 D). Similar to their counterpart in the spleen, LN subcapsular sinus macrophages were intact in DT-treated zDC-DTR mice and reduced in CD11c-DTR mice (Fig. 5 E). Therefore, DT-treated zDC-DTR mice maintain spleen and LN macrophage populations, whereas DT treatment in CD11c-DTR mice results in a substantial loss of multiple macrophage populations. In conclusion, zDC-DTR is equivalent to CD11c-DTR in cDC ablation but spares CD11c-expressing non-cDC populations affected by DT treatment in CD11c-DTR mice in both the steady state and during inflammation, most notably cells of the monocyte/macrophage lineage.

Immune responses in DT-treated zDC-DTR and CD11c-DTR mice

To examine the relative contribution of cDCs and other CD11c-expressing cells to immune responses, we compared DT-treated zDC- and CD11c-DTR bone marrow chimeras. As expected, DT treatment of zDC- and CD11c-DTR bone marrow chimeras before immunization with soluble OVA abrogated OT-I and OT-II proliferative responses (Fig. 6 A). Similarly, splenocytes from DT-treated zDC- and CD11c-DTR mice failed to stimulate allogeneic T cell proliferation in mixed leukocyte reactions (MLRs) in vitro (Fig. 6 B). Thus, cDCs are the primary cells required for antigen presentation to transferred OTI and OTII cells as well as stimulation of the MLR in vitro.

To determine the role of cDCs during the initiation of primary T_H1 responses, we compared immune responses to HIV-GAGp24 targeted with either α -DEC-205 or α -Treml4 in DT-treated zDC-DTR bone marrow chimeras. Mice were immunized with either α -DEC-205-GAGp24 to target CD8⁺DEC205⁺ cDCs and activated B cells, or with α -Treml4-GAGp24 to target cDCs and macrophages (Inaba et al., 1995; Hemmi et al., 2009, 2012). DT treatment abrogated antigen-specific T_H1 CD4⁺ T cell responses to both immunogens as measured by IFN- γ , IL-2, and TNF production after restimulation with GAGp24 in vitro (Fig. 6, C and D; and not depicted). We conclude that cDCs are the primary initiators of T_H1 immune responses after HIV-GAGp24 immunization irrespective of whether the antigen is also targeted to B cells or macrophages.

We next examined immunity to pathogen challenge with *Toxoplasma gondii*. Clearance of this protozoan parasite depends on IFN- γ production by CD4⁺ T cells (Denkers and Gazzinelli, 1998; Subauste and Remington, 2001; Lieberman and Hunter, 2002). zDC- and CD11c-DTR bone marrow chimeras were injected with DT 1 d before infection and every 3rd d thereafter. 8 d after *T. gondii* infection, we measured IFN- γ production by CD4⁺ T cell by flow cytometry and pathogen burden in the lung by Q-PCR. cDC depletion was equivalent in DT-treated zDC- and CD11c-DTR bone marrow chimeras 8 d after *T. gondii* infection (Fig. 6 E). Furthermore, IFN- γ CD4⁺ T cells were detectable but significantly reduced in the mLNs and spleens of both types of mice

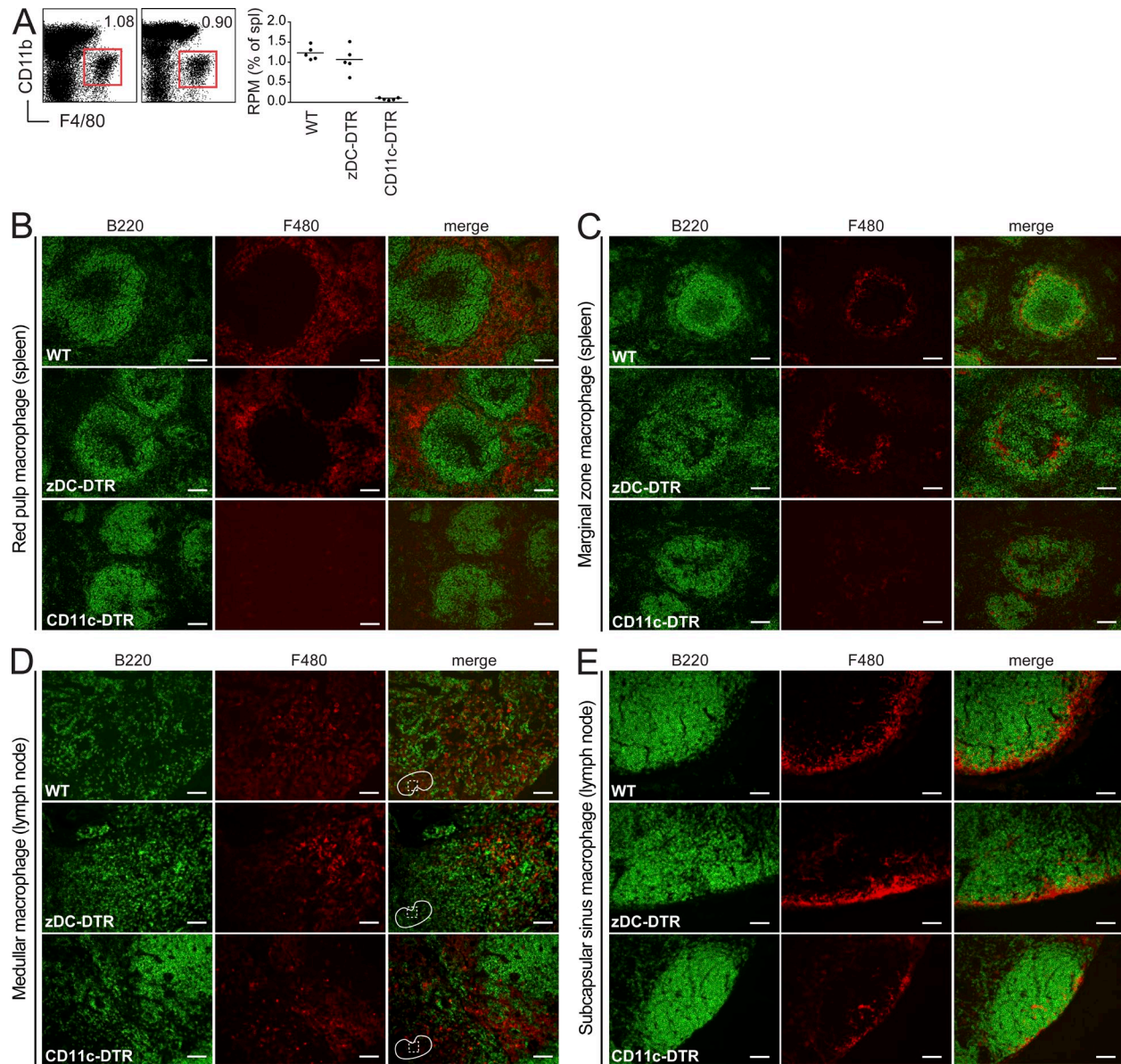


Figure 5. Macrophage populations in the spleen and skLNs are intact after DT injection in zDC-DTR mice. (A) Splenic $\text{Lin}^- \text{CD11c}^{\text{int}} \text{CD11b}^{\text{lo}} \text{F4}/80^+$ red pulp macrophages measured by flow cytometry in PBS- or DT-treated zDC-DTR bone marrow chimeras. Results are representative of three independent experiments with each point on the graph representing one mouse and the horizontal bars representing the means. (B–E) Spleen and skLNs from DT-treated WT, zDC-DTR, and CD11c-DTR mice were stained with B220 (green) to visualize B cell zones and appropriate macrophage markers (red). Bars, 100 μm . In the spleen, F4/80 identifies red pulp macrophages (B) and CD169 $^+$ marginal zone macrophages (C) which outline B cell zones. (D) F4/80 $^+$ medullar macrophages in the skLN. Diagram of LN included with merged image to represent region of LN imaged (dashed box) relative to entire LN (solid outline). (E) CD169 $^+$ subcapsular sinus macrophages located on the outer border of LN sections. Images represent results from three independent sets of experiments.

(Fig. 6 F and not depicted). However, the reduction was more profound in CD11c- than in zDC-DTR bone marrow chimeras. Accordingly, CD11c-DTR bone marrow chimeras displayed higher pathogen burdens than zDC-DTR bone marrow chimeras (Fig. 6 G), indicating that CD11c-DTR bone marrow chimeras mounted decreased overall levels of immunity to the pathogen. We conclude that DT treatment in CD11c-DTR mice impairs immune responses to *T. gondii* infection more so than in zDC-DTR.

To examine the role of cDCs and other CD11c-expressing cells in antitumor immune responses, zDC- and CD11c-DTR bone marrow chimeras were vaccinated with replication-deficient OVA-expressing adenovirus (Ad-OVA) and challenged 30 d later with MO4 (OVA-expressing B16 melanoma). cDC ablation was maintained for 2 wk after Ad-OVA immunization, and neither zDC- nor CD11c-DTR bone marrow chimeras showed any adverse side effects during this extended DT treatment. After challenge with MO4 melanoma,

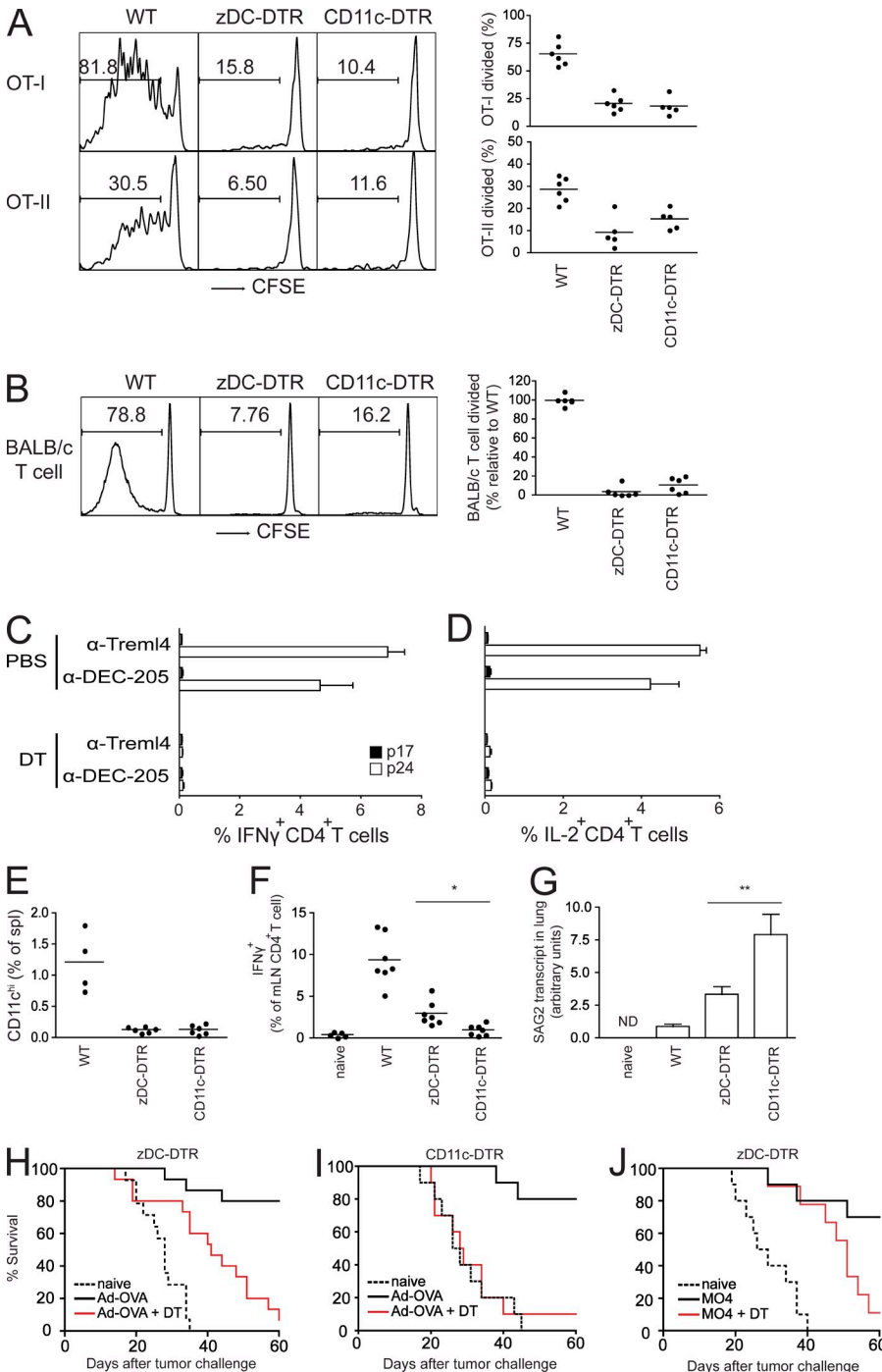


Figure 6. Comparison of DT treatment in zDC- and CD11c-DTR bone marrow chimeras during immune responses. (A) CFSE-labeled CD45.1⁺ OT-I and OT-II cells were transferred into CD45.2⁺ recipients, treated with DT 24 h later, and injected with 20 μ g OVA i.v. another 24 h later. CFSE dilution of CD45.1⁺ OT-I and OT-II cells was measured by flow cytometry 3 d after OVA injection. These experiments were repeated twice with two to three mice per group per experiment. The horizontal bar shows the mean per group. (B) 500,000 bulk splenocytes from DT-treated CD45.2⁺ C57BL/6 bone marrow chimeras were co-cultured with 50,000 CFSE-labeled CD45.1⁺ BALB/c T cells. CFSE dilution of CD45.1⁺ BALB/c T cells was measured by flow cytometry after 5 d. Results represent three experiments with two mice per group per experiment. The horizontal bar shows the mean per group. (C and D) PBS- and DT-treated zDC-DTR bone marrow chimeras were immunized with poly I:C plus α -CD40 and α -DEC-205-GAGp24 or α -Treml4-GAGp24, and IFN- γ and IL-2 production by splenic CD3⁺CD4⁺ T cells was measured after restimulation in vitro with p24 or p17 control peptide. This was repeated twice with four to five mice per group per experiment. Error bars indicate SEM. (E–G) Mice were treated with DT before infection with 15 *T. gondii* cysts by gavage and DT ablation was maintained until 8 d after infection when mice were euthanized. (E) The abundance of Lin⁻CD11c^{hi} cDCs in the spleens from DT-treated *T. gondii*-infected WT, zDC-DTR, and CD11c-DTR bone marrow chimeras determined by flow cytometry. (F) The percentage of CD3⁺CD4⁺ T cells producing IFN- γ in the mLN quantified by intracellular cytokine staining after restimulation in vitro. Uninfected mice were included as naive controls. Statistical significance was determined using a Student's *t* test. Results were pooled from three experiments with two to three mice per group per experiment. The horizontal bar shows the mean of each group. (G) Q-PCR of whole lung cDNA for *T. gondii* tachyzoite-specific SAG2 expression normalized to GAPDH. Uninfected mice were included as naive controls. ND indicates not detected. Error bars indicate SEM. Statistical significance was determined by Student's *t* test: * $P < 0.01$; ** $P < 0.005$.

significance was determined by Student's *t* test: * $P < 0.01$; ** $P < 0.005$. (H and I) Mice were injected with DT before i.v. immunization with Ad-OVA plus poly I:C and α -CD40, and DT ablation was maintained for 15 d. 1 mo after immunization, mice were challenged with 10⁵ MO4 cells i.v. and followed for survival. Each group contained 5–10 mice per group per experiment and was repeated three times. (J) As in H, but immunization was with 20 \times 10⁶ irradiated MO4 melanoma cells (7,500 rad) plus poly I:C and α -CD40, and challenge was with 10⁵ MO4 cells s.c. 1 mo later. The experiment was repeated twice with five mice per group per experiment.

zDC- and CD11c-DTR bone marrow chimeras that had received DT at the time of immunization did not survive as long as untreated controls (Fig. 6, H and I). However, DT-treated zDC-DTR bone marrow chimeras survived longer

than control mice receiving no vaccination, indicating a significant residual immune response to the tumor. Similar results were obtained by immunization with irradiated MO4 cells instead of Ad-OVA, and therefore the results are not

specific to immunization with adenovirus (Fig. 6 J). In contrast, DT-treated CD11c-DTR bone marrow chimeras survived only as long as unvaccinated control mice (Fig. 6 I). The number of OVA-specific CD8⁺ T cells 30 d after Ad-OVA immunization did not correlate with the duration of survival after MO4 melanoma challenge because both DTR models demonstrated similar defects in this population. Similarly, the number of lung tumor nodules was not different in zDC- and CD11c-DTR bone marrow chimeras that had received DT treatment at the time of Ad-OVA immunization when the mice were euthanized after losing 20% of their initial body weight. Therefore, DT treatment in CD11c-DTR prevents the development of antitumor memory responses, but immune responses are partially spared in DT-treated zDC-DTR mice.

DISCUSSION

zDC is an evolutionarily conserved, previously uncharacterized zinc finger transcription factor expressed specifically by cDCs and their immediate precursors but not by monocytes or other bone marrow-derived cells. We have inserted a human DTR cDNA into the 3'UTR of the zDC gene such that cell surface DTR expression is a reporter of zDC expression, and DT injection results in specific ablation of cDCs throughout the organism.

DC ablation in CD11c-DTR mice has been used extensively to study the role of DCs in immune responses *in vivo*. This was first accomplished by Jung et al. (2002), who used CD11c-DTR mice to demonstrate that DCs are responsible for cross-presentation of cell-associated OVA, and for priming cytotoxic T cell responses to *L. monocytogenes* and *Plasmodium yoelii*. CD11c-DTR mice have also been used to study immunity to many viral and bacterial pathogens including HSV-I (Kassim et al., 2006), *Mycobacterium tuberculosis* (Tian et al., 2005), and *T. gondii* (Liu et al., 2006). However, DT ablation is not entirely specific in CD11c-DTR mice because many leukocytes other than DCs also express CD11c (Probst et al., 2005; Zammit et al., 2005; Bennett and Clausen, 2007; Bradford et al., 2011). For example, macrophages are sensitive to DT ablation in CD11c-DTR mice, and these cells have also been implicated in the restimulation of primed T cells (Mellman et al., 1998; Trombetta and Mellman, 2005; Landsman and Jung, 2007) as well as the control of viral and bacterial infections (Aderem and Underhill, 1999; Gordon and Taylor, 2005). In addition, CD11c is expressed on populations of resting and activated monocytes, NK cells, and pDCs, and these populations are partially ablated by DT treatment in CD11c-DTR mice. In contrast, all of these CD11c-expressing non-cDCs were resistant to DT treatment in zDC-DTR. Therefore, zDC-DTR can be used to study the role of cDCs as opposed to CD11c-expressing cells in immunity.

There are two major subpopulations of cDCs in lymphoid and nonlymphoid organs: CD8⁺/CD103⁺ and CD8[−]/CD103[−] (Hashimoto et al., 2011). These two subsets originate from the same pre-DC precursor (Naik et al., 2006; Ginhoux et al., 2009; Helft et al., 2010) but differ in their antigen-presenting activities. CD8⁺/CD103⁺ cDCs are specialized

for cross-presentation, whereas CD8[−]/CD103[−] cDCs are more efficient at presenting antigens on MHCII (Dudziak et al., 2007; Kamphorst et al., 2010). Although there is no specific genetic tool for depleting CD8[−]/CD103[−] cDCs, loss of the transcription factor Batf3 results in specific loss of CD8⁺/CD103⁺ cDCs and Batf3^{−/−} mice have been used to investigate the relative roles of the two types of cDCs in immune responses (Hildner et al., 2008). Batf3^{−/−} mice are unable to cross-present cell-associated antigens or mount CD8⁺ T cell responses to West Nile Virus (WNV) but produce normal anti-WNV antibody and CD4⁺ T cell responses. Although Batf3^{−/−} mice show significant defects in antitumor immunity, they can still develop some tumor-specific CTL responses (Hildner et al., 2008). Finally, their IL-12 and CD8⁺ T cell responses to *T. gondii* were decreased but not completely abrogated. Whether these residual immune responses in Batf3^{−/−} mice were a result of CD8[−]/CD103[−] cDCs or other antigen-presenting cells, including macrophages (Gazzinelli et al., 1994), could not be determined in part because CD11c-DTR is not entirely cDC specific.

We included CD11c-DTR in our characterization of zDC-DTR mice to compare which populations of myeloid cells are ablated in each of the two models, and how these differences impact immune responses. Interestingly, similar to CD11c-DTR mice, DT treatment in zDC-DTR knockin mice is lethal, which necessitates the use of bone marrow chimeras for long-term experiments. Lethality in zDC-DTR knockin mice is most likely a result of the expression of zDC in some nonhematopoietic population because C57BL/6 → zDC-DTR bone marrow chimeras also die 24–48 h after DT injection. zDC-DTR → C57BL/6 bone marrow chimeras, however, survive continued DT treatment for up to 2 wk without adverse side effects.

zDC-DTR mice provide a model to ablate pre-DC-derived cDCs while sparing phenotypically similar monocyte-derived populations. In contrast, both cDCs and monocyte-derived macrophages/activated monocytes are sensitive to DT ablation in CD11c-DTR mice. Our comparison of DT-treated zDC- and CD11c-DTR mice confirmed that the absence of antigen presentation to transgenic T cells (Steinman, 2007) and stimulation of the MLR (Steinman and Witmer, 1978) is a result of cDC depletion. DT treatment preceding OVA immunization abrogated OT-I and OT-II responses in both zDC- and CD11c-DTR bone marrow chimeras. Similarly, splenocytes from both types of DT-treated mice failed to induce allogeneic T cell proliferation in MLRs. Furthermore, the loss of T_H1 CD4⁺ T cell responses after immunization with DEC-205- or Treml4-targeted antigen with poly I:C and α-CD40 in DT-treated zDC-DTR bone marrow chimeras demonstrates the importance of cDCs in priming these responses. Although B cells and macrophages are also targeted with antigen by α-DEC-205-GAGp24 and α-Treml4-GAGp24, respectively (Inaba et al., 1995; Hemmi et al., 2009, 2012), these populations were not sufficient to prime detectable T_H1 responses in DT-treated zDC-DTR mice.

However, there were significant differences between DT-treated zDC- and CD11c-DTR bone marrow chimeras in the steady state and during infection or immunization. For example, DT treatment in both zDC-DTR and CD11c-DTR results in impaired IFN- γ responses by CD4 $^+$ T cells during *T. gondii* infection, but zDC-DTR bone marrow chimeras showed significant residual immune responses despite the absence of cDCs. zDC-DTR mice produced more IFN γ $^+$ CD4 $^+$ T cells and suffered lower pathogen burden relative to CD11c-DTR. IL-12 is necessary to induce T_H1 IFN- γ responses to *T. gondii* (Gazzinelli et al., 1994; Yap et al., 2000), and CD8 $^+$ cDCs are required for optimal IL-12-dependent T_H1 responses in vivo (Liu et al., 2006; Mashayekhi et al., 2011). Nevertheless, cDC-deficient mice were able to mount a significant immune response. Irrespective of mechanism, our results confirm that cDCs are critical to induce optimal IFN- γ production by CD4 $^+$ T cells but suggest that additional CD11c $^+$ non-cDCs, possibly gut-resident CD11b $^+$ DCs, macrophages (Gazzinelli et al., 1994), activated monocytes, pDCs, or NK cells, can also contribute to *T. gondii* responses.

Likewise, zDC- and CD11c-DTR differed in their ability to produce protective immunity against MO4 melanoma. Whereas CD11c-DTR bone marrow chimeras were entirely unable to respond, zDC-DTR bone marrow chimeras mounted a significant immune response and survived longer than DT-treated CD11c-DTR or unimmunized controls. Therefore, a CD11c $^+$ non-cDC accessory population present during immunization in zDC-DTR, but absent in CD11c-DTR, can contribute to the initiation of antitumor immunity after immunization with Ad-OVA or MO4.

In conclusion, we have generated a new DTR model in which cDCs can be ablated while sparing other CD11c-expressing cells. By comparing zDC- and CD11c-DTR bone marrow chimeras, we show that CD11c-expressing, bone marrow-derived non-cDCs can contribute to the initiation of immunity against tumors and parasites.

MATERIALS AND METHODS

Microarray. MDP, CDP, pre-DC, and monocytes were isolated from the bone marrow of C57BL/6 mice. Total RNA extraction and hybridization on MOE-430 2.0 arrays (Affymetrix) were performed at Memorial Sloan-Kettering Cancer Center, New York, NY. Microarray data were analyzed using GeneSpring 10.0 software (Affymetrix). Triplicates of each population were collected and averaged in Genespring. MDP, CDP, pre-DC, and monocyte gene array data (GEO accession no.: GSE37566) were compared with previously obtained splenic B cell, T cell, and differentiated cDC array data (GEO accession no.: GSE6259; Dudziak et al., 2007).

Cell isolation. MP (Lin $^-($ CD3 $^-$ CD19 $^-$ NK1.1 $^-$ CD45R $^-$) CD11b $^+$ CD11c $^-$ Sca-1 $^-$ CD115 $^+$ Flt3 $^+$ CD117 hi), MDP (Lin $^-($ CD11b $^+$ CD11c $^-$ Sca-1 $^-$ CD115 $^+$ Flt3 $^+$ CD117 hi), CDP (Lin $^-($ CD11b $^+$ CD11c $^-$ Sca-1 $^-$ CD115 $^+$ Flt3 $^+$ CD117 lo), and cDC precursor (pre-DC, Lin $^-($ I-A/E $^-$ CD11c $^+$ Flt3 $^+$ CD172 α^{int}) were sorted from bone marrow of C57/Bl6 mice after MACS enrichment with Flt3-biotin and anti-biotin microbeads. Similarly, monocytes (Lin $^-$ CD11c $^-$ Ly6G $^-$ CD11b $^+$ CD115 $^+$ Ly6C hi) were sorted from bone marrow of C57BL/6 mice after MACS enrichment with CD115-biotin and anti-biotin microbeads. CD8 α^+ cDCs (CD8 α^+ cDC, Lin $^-$ CD11c hi I-A/E $^+$ CD8 α^+), CD11b $^+$ cDC (Lin $^-$ CD11c hi I-A/E $^+$ CD11b $^+$), and pDCs (CD3 $^-$ CD19 $^-$ NK1.1 $^-$ CD11c int CD45R $^+$) were sorted from spleen of C57/Bl6 mice after MACS enrichment with CD11c microbeads.

Antibodies and other reagents. The following reagents were from BD or eBioscience: anti-CD16-CD32 (2.4G2), anti-I-A/I-E (M5/114.15.2), anti-CD45R (RA3-6B2), anti-CD115 (AFS98), anti-Flt3 (A2F10), anti-CD3 (145-2C11), anti-CD4 (L3T4), anti-CD8 (53-6.7), anti-CD19 (1D3), anti-NK1.1 (PK136), anti-Ter119 (TER-119), anti-Sca-1 (D7), anti-CD11b (M1/70), anti-CD103 (2E7), anti-CD45.2 (104), anti-CD45.1 (A20), anti-CD14 (Sa2-8), anti-CD169 (MOMA-1), anti-F4/80 (BM8), anti-CD11c (N418), anti-CD172 α (P84), anti-CD117 (2B8), anti-PDCA-1 (eBio927), anti-Ly6C (HK1.4), anti-Ly6G (1A8), and anti-IFN- γ (XMG1.2). Anti-DEC-205 (NLDC145) was produced and provided by C. Cheong. Biotin-conjugated anti-hDTR (hHB-EGF; R&D Systems) was used at a final concentration of 1 μ g/ml in PBS containing 2% FBS and 0.1% sodium azide, and streptavidin-PE (eBioscience) was used as a secondary.

Pharm Lyse lysing buffer, Cytoperm/Cytofix solution, and Perm/Wash buffer were purchased from BD. Anti-biotin, anti-CD11c, and anti-CD11b microbeads, and pDC isolation kit, were from Miltenyi Biotec. Other reagents included PBS, HBSS, FBS, ACK lysis buffer, and EDTA (Invitrogen), Collagenase D (Roche) for spleen, skLN, mLN, lung, and liver digestion (Ginhoux et al., 2009; Liu et al., 2009), and Collagenase VIII (Sigma-Aldrich) for small intestine digestion (Mucida et al., 2007).

Quantitative real-time PCR. Total RNA was isolated from at least 5×10^4 FACS-sorted C57BL/6 primary cells with TRIzol (Invitrogen), from which cDNA libraries were reverse transcribed using Superscript II (Invitrogen) and random primers. Murine zDC (Zbtb46) cDNA was amplified with primers in exon 4 (forward: 5'-TCACATACTGGAGAGCGGC-3') and exon 5 (reverse: 5'-CCTCATCCTCATCCTCAACC-3'). GAPDH cDNA was also amplified to normalize zDC mRNA levels (forward: 5'-TGAAGCAG-GCATCTGAGGG-3'; reverse: 5'-CGAAGGTGGAAGAGTGGGAG-3'). All quantitative PCR reactions were performed with Brilliant SYBR Green (Agilent Technologies) on an Mx3005P system (Agilent Technologies).

Monoclonal antibody. Recombinant mouse zDC was produced as fusion protein to GST in BL21 competent cells (Promega) transformed with pGEX-6p-1 vector (GE Healthcare) containing the mouse zDC cDNA sequence. Glutathione Sepharose beads and PreScission Protease (GE Healthcare) were used to purify zDC without the GST tag using the manufacturer's protocols.

Armenian hamsters were immunized with recombinant mouse zDC to produce specific antibodies by the Monoclonal Antibody Core Facility at Memorial Sloan-Kettering Cancer Center. Hybridomas were serially diluted and screened for zDC reactivity by ELISA. Antibodies were purified from hybridoma supernatants with Protein G (GE Healthcare).

Dendrogram. Mouse (NP_081932.1), rat (NP_001101278.1), human (NP_079500.2), chimpanzee (XP_003317118.1), macaque (XP_001084247.1), cow (NP_001179093.1), chicken (XP_417431.2), frog (NP_001087165.1), zebra fish (XP_699124.4), and pufferfish (CAG11269.1) protein sequences were acquired from the NCBI protein sequence database and were assembled into a neighbor joining tree using MacVector software.

Mice. zDC-DTR knockin mice were generated by homologous recombination in C57BL/6 albino embryonic stem cells at The Rockefeller University Gene Targeting Resource Center and maintained on a C57BL/6 background. The targeting construct, assembled by PCR and cloning, consisted of two arms of homology—one 1.97-kb fragment spanning intron 4 up to the stop codon located in exon 5, and a second 8.25-kb fragment containing the 3'UTR of exon 5 and intergenic sequence—introduced into the pCON-ACN vector.

C57BL/6, C57BL/6.SJL, and CD11c-DTR mice were purchased from The Jackson Laboratory. Bone marrow chimeras were reconstituted for at least 8–10 wk after lethal irradiation (two doses of 525 rad, 3 h apart) and i.v. transfer of $5-10 \times 10^6$ bone marrow cells. zDC $^{+/DTR}$ and CD11c-DTR hemizygous mice were bred at The Rockefeller University for use in experiments and as bone marrow donors. C57BL/6 mice purchased from The Jackson Laboratory were used as controls in experiments and as control bone

marrow donors. All mice were housed in The Rockefeller University Comparative Bioscience Center under specific pathogen-free conditions. All experiments were performed in accordance with National Institutes of Health guidelines and approved by The Rockefeller University Animal Care and Use Committee.

DT. DT was purchased from Sigma-Aldrich, and every new batch of DT was titrated in zDC-DTR mice, due to variability between batches, to determine the lowest effective dose and limit DT toxicity. For transient DT ablation, C57BL/6 (WT) and zDC-DTR bone marrow chimeras were injected i.p. with 20 ng DT per gram of body weight, whereas CD11c-DTR bone marrow chimeras received 4 ng DT per gram. Mice were euthanized 12–24 h after DT injection for analysis. To maintain DT ablation, mice received 4 ng DT per gram of body weight on the 3rd d after the initial DT injection and every 3rd d thereafter.

L. monocytogenes. WT, zDC-DTR, and CD11c-DTR bone marrow chimeras were infected i.v. with 5×10^4 *L. monocytogenes* CFU and injected with DT i.p. 24–48 h after infection. Spleens were collected 12 h after DT injection and the abundance of CD11b⁺Ly6C⁺CD11c⁺MHCII⁺ activated monocytes was determined by flow cytometry.

Immunofluorescent staining. Tissues were fixed in 3% PFA/25% sucrose overnight, frozen in O.C.T Compound (Tissue-Tek; Sakura), and stored at -80°C . Frozen tissue was cut into 20- μm -thick sections, fixed for 10 min in ice-cold acetone, and rehydrated in PBS for 30 min. Tissue sections were outlined with a Pap pen and stained for 2 h at room temperature in 1% FCS in PBS. Antibody cocktail contained anti-CD16/CD32 blocking Ab (2.4G2, 1:100; BD), FITC anti-CD45R/B220 (RA3-6B2, 1:200; BD), and either APC anti-F4/80 (BM8, 1:100; eBioscience) or Alexa Fluor 647 anti-CD169 (MOMA-1, 1:100; AbD Serotec). Sections were washed for 10 min three times and mounted using ProLong Gold Antifade Reagent with DAPI (Invitrogen). Images were acquired on a wide-field fluorescent microscope (Carl Zeiss) using MetaVue acquisition software (Molecular Devices) and a digital camera (Orca ER B/W; Hamamatsu Photonics) at the Rockefeller University Bio-Imaging Resource Center.

OT-I and OT-II proliferation in vivo. $2-5 \times 10^6$ CD45.1⁺ OT-I and OT-II cells purified with CD8⁺ T cell and CD4⁺ T cell isolation kits (Miltenyi Biotec), respectively, were labeled with 2 μM CFSE for 10 min at 37°C and transferred i.v. into CD45.2⁺ WT, zDC-DTR, and CD11c-DTR bone marrow chimeras. The mice were treated with DT 24 h after T cell transfer, and received 20 μg LPS-free soluble OVA (Sigma-Aldrich) i.v. another 24 h after DT treatment. 3 d after OVA immunization, spleens and skLNs were collected to analyze CFSE dilution of transferred CD45.1⁺ OT-I and OT-II cells by flow cytometry.

MLR. 5×10^5 bulk CD45.2⁺ C57BL/6 splenocytes from DT-treated WT, zDC-DTR, and CD11c-DTR bone marrow chimeras were co-cultured in complete RPMI with 5×10^4 CFSE-labeled T cells isolated by negative selection with Dynabeads (Invitrogen) from CD45.1⁺ BALB/c mice. CFSE dilution caused by proliferation of BALB/c T cells was measured by flow cytometry after 5 d in vitro. Bulk CD45.2⁺ C57BL/6 splenocytes were lethally irradiated (1,000 rad) before co-culture.

Antigen-targeted immunization. zDC-DTR bone marrow chimeras received DT 24 h before immunization and DT ablation was maintained for 14 d. Mice were immunized with 5 μg α -DEC-205-GAGp24 or α -Treml4-GAGp24, plus 50 μg poly I:C and 25 μg α -CD40. Bulk splenocytes were restimulated 14 d later in complete RPMI plus 5 $\mu\text{g}/\text{ml}$ brefeldin A (Sigma-Aldrich) with p24 or p17 in vitro, and the production of IFN- γ , TNF, and IL-2 were measured in CD3⁺CD4⁺ T cells by intracellular cytokine staining (ICS).

T. gondii. 24 h after DT treatment, WT, zDC-DTR, and CD11c-DTR bone marrow chimeras were infected with 15 *T. gondii* cysts by gavage in

whole brain lysates from *T. gondii*-infected mice. During the course of infection, mice received DT every 3rd d to maintain ablation.

After 8 d of infection, the mLNs and spleens of the infected mice were collected for analysis. Single cell suspensions were restimulated at 10^7 cells/ml in vitro with 50 ng/ml PMA and 500 ng/ml ionomycin (Sigma-Aldrich) and GolgiStop (BD) in complete RPMI for 5 h, and the proportion of CD4⁺ T cells producing IFN- γ was determined by ICS.

For *T. gondii* pathogen quantification, whole lung was homogenized in TRIzol (Invitrogen) to extract RNA for cDNA synthesis as described earlier. SAG2 levels were quantified by RT-PCR (Subauste and Remington, 2001) and normalized to GAPDH as before.

Ad-OVA and MO4 immunization. 24 h after DT treatment, zDC-DTR and CD11c-DTR bone marrow chimeras were immunized with 10^7 PFU replication-deficient Ad-OVA i.m. or 20×10^6 irradiated (7,500 rad) MO4 i.v. with 50 μg poly I:C and 50 μg α -CD40. To maintain ablation, mice received DT every 3rd d for 15 d. 30 d after immunization (i.e., 15 d after the final DT injection), mice were challenged with 10^5 MO4 either i.v. or s.c. (for Ad-OVA or irradiated MO4 immunization, respectively). The OVA-transfected MO4 cells were provided by R. Steinman (Rockefeller University, New York, NY) and were cultured in DME plus 10% FCS and 100 U/ml penicillin-streptomycin (Invitrogen). Mice were monitored after MO4 challenge and euthanized when they had lost 20% of their starting body weight.

We are grateful to members of the Nussenzweig laboratory for helpful discussion, reagents, or critical reading of the manuscript.

This work was supported in part by National Institutes of Health (NIH) grant number AI051573. M.C. Nussenzweig is an HHMI investigator. M.M. Meredith was supported by an NIH Immunity and Infectious Disease Training Grant. K. Liu was supported by Dana Neuroimmunology grant and a Pilot Grant funded by P30 AR044535/AR/NIAMS/NIH Columbia University Medical Center Skin Disease Research Center.

The authors report no competing financial interests.

Submitted: 16 December 2011

Accepted: 2 May 2012

REFERENCES

- Aderem, A., and D.M. Underhill. 1999. Mechanisms of phagocytosis in macrophages. *Annu. Rev. Immunol.* 17:593–623. <http://dx.doi.org/10.1146/annurev.immunol.17.1.593>
- Banchereau, J., and R.M. Steinman. 1998. Dendritic cells and the control of immunity. *Nature*. 392:245–252. <http://dx.doi.org/10.1038/32588>
- Bennett, C.L., and B.E. Clausen. 2007. DC ablation in mice: promises, pitfalls, and challenges. *Trends Immunol.* 28:525–531. <http://dx.doi.org/10.1016/j.it.2007.08.011>
- Bogunovic, M., F. Ginhoux, J. Helft, L. Shang, D. Hashimoto, M. Greter, K. Liu, C. Jakubzick, M.A. Ingersoll, M. Leboeuf, et al. 2009. Origin of the lamina propria dendritic cell network. *Immunity*. 31:513–525. <http://dx.doi.org/10.1016/j.immuni.2009.08.010>
- Bradford, B.M., D.P. Sester, D.A. Hume, and N.A. Mabbott. 2011. Defining the anatomical localisation of subsets of the murine mononuclear phagocyte system using integrin alpha X (Itgax, CD11c) and colony stimulating factor 1 receptor (Csf1r, CD115) expression fails to discriminate dendritic cells from macrophages. *Immunobiology*. 216:1228–1237. <http://dx.doi.org/10.1016/j.imbio.2011.08.006>
- Cheong, C., I. Matos, J.H. Choi, D.B. Dandamudi, E. Shrestha, M.P. Longhi, K.L. Jeffrey, R.M. Anthony, C. Kluger, G. Nchinda, et al. 2010. Microbial stimulation fully differentiates monocytes to DC-SIGN/CD209(+) dendritic cells for immune T cell areas. *Cell*. 143:416–429. <http://dx.doi.org/10.1016/j.cell.2010.09.039>
- Denkers, E.Y., and R.T. Gazzinelli. 1998. Regulation and function of T-cell-mediated immunity during *Toxoplasma gondii* infection. *Clin. Microbiol. Rev.* 11:569–588.
- Dudziak, D., A.O. Kamphorst, G.F. Heidkamp, V.R. Buchholz, C. Trumppfeller, S. Yamazaki, C. Cheong, K. Liu, H.W. Lee, C.G. Park, et al. 2007. Differential antigen processing by dendritic cell subsets in vivo. *Science*. 315:107–111. <http://dx.doi.org/10.1126/science.1136080>

Fogg, D.K., C. Sibon, C. Miled, S. Jung, P. Aucouturier, D.R. Littman, A. Cumano, and F. Geissmann. 2006. A clonogenic bone marrow progenitor specific for macrophages and dendritic cells. *Science*. 311:83–87. <http://dx.doi.org/10.1126/science.1117729>

Gazzinelli, R.T., M. Wysocka, S. Hayashi, E.Y. Denkers, S. Hieny, P. Caspar, G. Trinchieri, and A. Sher. 1994. Parasite-induced IL-12 stimulates early IFN-gamma synthesis and resistance during acute infection with *Toxoplasma gondii*. *J. Immunol.* 153:2533–2543.

Geissmann, F., S. Jung, and D.R. Littman. 2003. Blood monocytes consist of two principal subsets with distinct migratory properties. *Immunity*. 19:71–82. [http://dx.doi.org/10.1016/S1074-7613\(03\)00174-2](http://dx.doi.org/10.1016/S1074-7613(03)00174-2)

Ginhoux, F., K. Liu, J. Helft, M. Bogunovic, M. Greter, D. Hashimoto, J. Price, N. Yin, J. Bromberg, S.A. Lira, et al. 2009. The origin and development of nonlymphoid tissue CD103⁺ DCs. *J. Exp. Med.* 206:3115–3130. <http://dx.doi.org/10.1084/jem.20091756>

Gordon, S., and P.R. Taylor. 2005. Monocyte and macrophage heterogeneity. *Nat. Rev. Immunol.* 5:953–964. <http://dx.doi.org/10.1038/nri1733>

Hashimoto, D., J. Miller, and M. Merad. 2011. Dendritic cell and macrophage heterogeneity in vivo. *Immunity*. 35:323–335. <http://dx.doi.org/10.1016/j.jimmuni.2011.09.007>

Helft, J., F. Ginhoux, M. Bogunovic, and M. Merad. 2010. Origin and functional heterogeneity of non-lymphoid tissue dendritic cells in mice. *Immunol. Rev.* 234:55–75. <http://dx.doi.org/10.1111/j.0105-2896.2009.00885.x>

Hemmi, H., J. Idoyaga, K. Suda, N. Suda, K. Kennedy, M. Noda, A. Aderem, and R.M. Steinman. 2009. A new triggering receptor expressed on myeloid cells (Trem) family member, Trem-like 4, binds to dead cells and is a DNAX activation protein 12-linked marker for subsets of mouse macrophages and dendritic cells. *J. Immunol.* 182:1278–1286.

Hemmi, H., N. Zaidi, B. Wang, I. Matos, C. Fiorese, A. Lubkin, L. Zbytniuk, K. Suda, K. Zhang, M. Noda, et al. 2012. Trem4, an Ig superfamily member, mediates presentation of several antigens to T cells in vivo, including protective immunity to HER2 protein. *J. Immunol.* 188:1147–1155. <http://dx.doi.org/10.4049/jimmunol.1102541>

Hildner, K., B.T. Edelson, W.E. Purtha, M. Diamond, H. Matsushita, M. Kohyama, B. Calderon, B.U. Schraml, E.R. Unanue, M.S. Diamond, et al. 2008. Batf3 deficiency reveals a critical role for CD8alpha⁺ dendritic cells in cytotoxic T cell immunity. *Science*. 322:1097–1100. <http://dx.doi.org/10.1126/science.1164206>

Hohl, T.M., A. Rivera, L. Lipuma, A. Gallegos, C. Shi, M. Mack, and E.G. Palmer. 2009. Inflammatory monocytes facilitate adaptive CD4 T cell responses during respiratory fungal infection. *Cell Host Microbe*. 6:470–481. <http://dx.doi.org/10.1016/j.chom.2009.10.007>

Inaba, K., W.J. Swiggard, M. Inaba, J. Meltzer, A. Mirza, T. Sasagawa, M.C. Nussenzweig, and R.M. Steinman. 1995. Tissue distribution of the DEC-205 protein that is detected by the monoclonal antibody NLDC-145. I. Expression on dendritic cells and other subsets of mouse leukocytes. *Cell. Immunol.* 163:148–156. <http://dx.doi.org/10.1006/cimm.1995.1109>

Iparraguirre, A., J.W. Tobias, S.E. Hensley, K.S. Masek, L.L. Cavanagh, M. Rendl, C.A. Hunter, H.C. Ertl, U.H. von Andrian, and W. Weninger. 2008. Two distinct activation states of plasmacytoid dendritic cells induced by influenza virus and CpG 1826 oligonucleotide. *J. Leukoc. Biol.* 83:610–620. <http://dx.doi.org/10.1189/jlb.0807511>

Jung, S., D. Unutmaz, P. Wong, G. Sano, K. De los Santos, T. Sparwasser, S. Wu, S. Vuthoori, K. Ko, F. Zavala, et al. 2002. In vivo depletion of CD11c⁺ dendritic cells abrogates priming of CD8⁺ T cells by exogenous cell-associated antigens. *Immunity*. 17:211–220. [http://dx.doi.org/10.1016/S1074-7613\(02\)00365-5](http://dx.doi.org/10.1016/S1074-7613(02)00365-5)

Kamphorst, A.O., P. Guermonprez, D. Dudziak, and M.C. Nussenzweig. 2010. Route of antigen uptake differentially impacts presentation by dendritic cells and activated monocytes. *J. Immunol.* 185:3426–3435. <http://dx.doi.org/10.4049/jimmunol.1001205>

Karsunky, H., M. Merad, A. Cozzio, I.L. Weissman, and M.G. Manz. 2003. Flt3 ligand regulates dendritic cell development from Flt3⁺ lymphoid and myeloid-committed progenitors to Flt3⁺ dendritic cells in vivo. *J. Exp. Med.* 198:305–313. <http://dx.doi.org/10.1084/jem.20030323>

Kassim, S.H., N.K. Rajasagi, X. Zhao, R. Chervenak, and S.R. Jennings. 2006. In vivo ablation of CD11c-positive dendritic cells increases susceptibility to herpes simplex virus type 1 infection and diminishes NK and T-cell responses. *J. Virol.* 80:3985–3993. <http://dx.doi.org/10.1128/JVI.80.8.3985-3993.2006>

Kohyama, M., W. Ise, B.T. Edelson, P.R. Wilker, K. Hildner, C. Mejia, W.A. Frazier, T.L. Murphy, and K.M. Murphy. 2009. Role for Spi-C in the development of red pulp macrophages and splenic iron homeostasis. *Nature*. 457:318–321. <http://dx.doi.org/10.1038/nature07472>

Landsman, L., and S. Jung. 2007. Lung macrophages serve as obligatory intermediate between blood monocytes and alveolar macrophages. *J. Immunol.* 179:3488–3494.

León, B., M. López-Bravo, and C. Ardavín. 2007. Monocyte-derived dendritic cells formed at the infection site control the induction of protective T helper 1 responses against Leishmania. *Immunity*. 26:519–531. <http://dx.doi.org/10.1016/j.jimmuni.2007.01.017>

Lieberman, L.A., and C.A. Hunter. 2002. The role of cytokines and their signaling pathways in the regulation of immunity to *Toxoplasma gondii*. *Int. Rev. Immunol.* 21:373–403. <http://dx.doi.org/10.1080/08830180213281>

Liu, C.H., Y.T. Fan, A. Dias, L. Esper, R.A. Corn, A. Bafica, F.S. Machado, and J. Aliberti. 2006. Cutting edge: dendritic cells are essential for in vivo IL-12 production and development of resistance against *Toxoplasma gondii* infection in mice. *J. Immunol.* 177:31–35.

Liu, K., and M.C. Nussenzweig. 2010. Origin and development of dendritic cells. *Immunol. Rev.* 234:45–54. <http://dx.doi.org/10.1111/j.0105-2896.2009.00879.x>

Liu, K., C. Waskow, X. Liu, K. Yao, J. Hoh, and M. Nussenzweig. 2007. Origin of dendritic cells in peripheral lymphoid organs of mice. *Nat. Immunol.* 8:578–583. <http://dx.doi.org/10.1038/ni1462>

Liu, K., G.D. Victora, T.A. Schwickert, P. Guermonprez, M.M. Meredith, K. Yao, F.F. Chu, G.J. Randolph, A.Y. Rudensky, and M. Nussenzweig. 2009. In vivo analysis of dendritic cell development and homeostasis. *Science*. 324:392–397. <http://dx.doi.org/10.1126/science.1170540>

Mashayekhi, M., M.M. Sandau, I.R. Dunay, E.M. Frickel, A. Khan, R.S. Goldszmid, A. Sher, H.L. Ploegh, T.L. Murphy, L.D. Sibley, and K.M. Murphy. 2011. CD8α(+) dendritic cells are the critical source of interleukin-12 that controls acute infection by *Toxoplasma gondii* tachyzoites. *Immunity*. 35:249–259. <http://dx.doi.org/10.1016/j.jimmuni.2011.08.008>

Mellman, I., S.J. Turley, and R.M. Steinman. 1998. Antigen processing for amateurs and professionals. *Trends Cell Biol.* 8:231–237. [http://dx.doi.org/10.1016/S0962-8924\(98\)01276-8](http://dx.doi.org/10.1016/S0962-8924(98)01276-8)

Mucida, D., Y. Park, G. Kim, O. Turovskaya, I. Scott, M. Kronenberg, and H. Cheroutre. 2007. Reciprocal TH17 and regulatory T cell differentiation mediated by retinoic acid. *Science*. 317:256–260. <http://dx.doi.org/10.1126/science.1145697>

Murphy, K.M. 2011. Comment on “Activation of β-catenin in dendritic cells regulates immunity versus tolerance in the intestine”. *Science*. 333:405, author reply :405. <http://dx.doi.org/10.1126/science.1198277>

Naik, S.H., A.I. Proietto, N.S. Wilson, A. Dakic, P. Schnorrer, M. Fuchsberger, M.H. Lahoud, M. O’Keeffe, Q.X. Shao, W.F. Chen, et al. 2005. Cutting edge: generation of splenic CD8⁺ and CD8⁻ dendritic cell equivalents in Fms-like tyrosine kinase 3 ligand bone marrow cultures. *J. Immunol.* 174:6592–6597.

Naik, S.H., D. Metcalf, A. van Nieuwenhuijze, I. Wicks, L. Wu, M. O’Keeffe, and K. Shortman. 2006. Intrasplenic steady-state dendritic cell precursors that are distinct from monocytes. *Nat. Immunol.* 7:663–671. <http://dx.doi.org/10.1038/ni1340>

Naik, S.H., P. Sathe, H.Y. Park, D. Metcalf, A.I. Proietto, A. Dakic, S. Carotta, M. O’Keeffe, M. Bahlo, A. Papenfuss, et al. 2007. Development of plasmacytoid and conventional dendritic cell subtypes from single precursor cells derived in vitro and in vivo. *Nat. Immunol.* 8:1217–1226. <http://dx.doi.org/10.1038/ni1522>

Nussenzweig, M.C., R.M. Steinman, B. Gutchinov, and Z.A. Cohn. 1980. Dendritic cells are accessory cells for the development of anti-trinitrophenyl cytotoxic T lymphocytes. *J. Exp. Med.* 152:1070–1084. <http://dx.doi.org/10.1084/jem.152.4.1070>

Nussenzweig, M.C., R.M. Steinman, J.C. Unkeless, M.D. Witmer, B. Gutchinov, and Z.A. Cohn. 1981. Studies of the cell surface of mouse dendritic cells and other leukocytes. *J. Exp. Med.* 154:168–187. <http://dx.doi.org/10.1084/jem.154.1.168>

Nussenzweig, M.C., R.M. Steinman, M.D. Witmer, and B. Gutchinov. 1982. A monoclonal antibody specific for mouse dendritic cells. *Proc. Natl. Acad. Sci. USA.* 79:161–165. <http://dx.doi.org/10.1073/pnas.79.1.161>

Onai, N., A. Obata-Onai, M.A. Schmid, T. Ohteki, D. Jarrossay, and M.G. Manz. 2007. Identification of clonogenic common Flt3+M-CSFR+ plasmacytoid and conventional dendritic cell progenitors in mouse bone marrow. *Nat. Immunol.* 8:1207–1216. <http://dx.doi.org/10.1038/ni1518>

Probst, H.C., K. Tschanen, B. Odermatt, R. Schwendener, R.M. Zinkernagel, and M. Van Den Broek. 2005. Histological analysis of CD11c-DTR/GFP mice after in vivo depletion of dendritic cells. *Clin. Exp. Immunol.* 141:398–404. <http://dx.doi.org/10.1111/j.1365-2249.2005.02868.x>

Randolph, G.J., K. Inaba, D.F. Robbiani, R.M. Steinman, and W.A. Muller. 1999. Differentiation of phagocytic monocytes into lymph node dendritic cells in vivo. *Immunity.* 11:753–761. [http://dx.doi.org/10.1016/S1074-7613\(00\)80149-1](http://dx.doi.org/10.1016/S1074-7613(00)80149-1)

Randolph, G.J., C. Jakubzick, and C. Qu. 2008. Antigen presentation by monocytes and monocyte-derived cells. *Curr. Opin. Immunol.* 20:52–60. <http://dx.doi.org/10.1016/j.co.2007.10.010>

Robbins, S.H., T. Walzer, D. Dembélé, C. Thibault, A. Defays, G. Bessou, H. Xu, E. Vivier, M. Sellars, P. Pierre, et al. 2008. Novel insights into the relationships between dendritic cell subsets in human and mouse revealed by genome-wide expression profiling. *Genome Biol.* 9:R17. <http://dx.doi.org/10.1186/gb-2008-9-1-r17>

Romani, N., S. Gruner, D. Brang, E. Kämpgen, A. Lenz, B. Trockenbacher, G. Konwalinka, P.O. Fritsch, R.M. Steinman, and G. Schuler. 1994. Proliferating dendritic cell progenitors in human blood. *J. Exp. Med.* 180:83–93. <http://dx.doi.org/10.1084/jem.180.1.83>

Sallusto, F., and A. Lanzavecchia. 1994. Efficient presentation of soluble antigen by cultured human dendritic cells is maintained by granulocyte/macrophage colony-stimulating factor plus interleukin 4 and downregulated by tumor necrosis factor alpha. *J. Exp. Med.* 179:1109–1118. <http://dx.doi.org/10.1084/jem.179.4.1109>

Sallusto, F., M. Cella, C. Danieli, and A. Lanzavecchia. 1995. Dendritic cells use macropinocytosis and the mannose receptor to concentrate macromolecules in the major histocompatibility complex class II compartment: downregulation by cytokines and bacterial products. *J. Exp. Med.* 182:389–400. <http://dx.doi.org/10.1084/jem.182.2.389>

Schmid, M.A., D. Kingston, S. Boddu, and M.G. Manz. 2010. Instructive cytokine signals in dendritic cell lineage commitment. *Immunol. Rev.* 234:32–44. <http://dx.doi.org/10.1111/j.0105-2896.2009.00877.x>

Schulz, C., E. Gomez Perdigero, L. Chorro, H. Szabo-Rogers, N. Cagnard, K. Kierdorf, M. Prinz, B. Wu, S.E. Jacobsen, J.W. Pollard, et al. 2012. A lineage of myeloid cells independent of Myb and hematopoietic stem cells. *Science.* 336:86–90. <http://dx.doi.org/10.1126/science.1219179>

Serbina, N.V., T.P. Salazar-Mather, C.A. Biron, W.A. Kuziel, and E.G. Pamer. 2003. TNF/iNOS-producing dendritic cells mediate innate immune defense against bacterial infection. *Immunity.* 19:59–70. [http://dx.doi.org/10.1016/S1074-7613\(03\)00171-7](http://dx.doi.org/10.1016/S1074-7613(03)00171-7)

Steinman, R.M. 2007. Lasker Basic Medical Research Award. Dendritic cells: versatile controllers of the immune system. *Nat. Med.* 13:1155–1159. <http://dx.doi.org/10.1038/nm1643>

Steinman, R.M., and Z.A. Cohn. 1973. Identification of a novel cell type in peripheral lymphoid organs of mice. I. Morphology, quantitation, tissue distribution. *J. Exp. Med.* 137:1142–1162. <http://dx.doi.org/10.1084/jem.137.5.1142>

Steinman, R.M., and M.D. Witmer. 1978. Lymphoid dendritic cells are potent stimulators of the primary mixed leukocyte reaction in mice. *Proc. Natl. Acad. Sci. USA.* 75:5132–5136. <http://dx.doi.org/10.1073/pnas.75.10.5132>

Subauste, C., and J. Remington. 2001. Animal models for *Toxoplasma gondii* infection. *Curr. Protoc. Immunol.* Chapter 19:Unit 19.3.

Tian, T., J. Woodworth, M. Sköld, and S.M. Behar. 2005. In vivo depletion of CD11c+ cells delays the CD4+ T cell response to *Mycobacterium tuberculosis* and exacerbates the outcome of infection. *J. Immunol.* 175:3268–3272.

Tittel, A.P., C. Heuser, C. Ohliger, C. Llanto, S. Yona, G.J. Hämmerling, D.R. Engel, N. Garbi, and C. Kurts. 2012. Functionally relevant neutrophilia in CD11c diphtheria toxin receptor transgenic mice. *Nat. Methods.* 9:385–390. <http://dx.doi.org/10.1038/nmeth.1905>

Trombetta, E.S., and I. Mellman. 2005. Cell biology of antigen processing in vitro and in vivo. *Annu. Rev. Immunol.* 23:975–1028. <http://dx.doi.org/10.1146/annurev.immunol.22.012703.104538>

Varol, C., L. Landsman, D.K. Fogg, L. Greenshtein, B. Gildor, R. Margalit, V. Kalchenko, F. Geissmann, and S. Jung. 2007. Monocytes give rise to mucosal, but not splenic, conventional dendritic cells. *J. Exp. Med.* 204:171–180. <http://dx.doi.org/10.1084/jem.20061011>

Varol, C., A. Vallon-Eberhard, E. Elinav, T. Aychek, Y. Shapira, H. Luche, H.J. Fehling, W.D. Hardt, G. Shakhar, and S. Jung. 2009. Intestinal lamina propria dendritic cell subsets have different origin and functions. *Immunity.* 31:502–512. <http://dx.doi.org/10.1016/j.immuni.2009.06.025>

Waskow, C., K. Liu, G. Darrasse-Jéze, P. Guermonprez, F. Ginhoux, M. Merad, T. Shengelia, K. Yao, and M. Nussenzweig. 2008. The receptor tyrosine kinase Flt3 is required for dendritic cell development in peripheral lymphoid tissues. *Nat. Immunol.* 9:676–683. <http://dx.doi.org/10.1038/ni.1615>

Yap, G., M. Pesin, and A. Sher. 2000. Cutting edge: IL-12 is required for the maintenance of IFN-gamma production in T cells mediating chronic resistance to the intracellular pathogen, *Toxoplasma gondii*. *J. Immunol.* 165:628–631.

Zaft, T., A. Sapoznikov, R. Krauthgamer, D.R. Littman, and S. Jung. 2005. CD11chigh dendritic cell ablation impairs lymphopenia-driven proliferation of naive and memory CD8+ T cells. *J. Immunol.* 175:6428–6435.

Zammit, D.J., L.S. Cauley, Q.M. Pham, and L. Lefrançois. 2005. Dendritic cells maximize the memory CD8 T cell response to infection. *Immunity.* 22:561–570. <http://dx.doi.org/10.1016/j.immuni.2005.03.005>